THE GRAVITY FIELD OF MARS

R. D. Reasenberg, I. I. Shapiro, R. D. White

Department of Earth and Planetary Sciences
Massachusetts Institute of Technology
Cambridge, Massachusetts 02139

Abstract. A complete sixth-degree spherical-harmonic model of the gravitational potential of Mars has been produced from an analysis of Doppler data obtained from the radio tracking of the Mariner-9 spacecraft for over 200 orbital revolutions. The equipotential surface defined by this model is estimated to be accurate to within 100 m below 60° North Latitude and to within 300 m above. The dominant feature of this surface is a Tharsis-related bulge which rises nearly two kilometers above the surrounding areas. Gravitational "lows" are found to correspond to the Hellas depression and the Valles Marineris.

Introduction

Knowledge of the gravitational potential of Mars provides strong constraints on models of its interior (Johnston et al., 1974). Questions of isostasy and depth of compensation, for example, can be answered only with the combination of topographic and gravitational information. Further, the accuracy of the Mariner-9 and Viking tests of general relativity that rely on ranging from Earth to a spacecraft in orbit about Mars rests in part on the accuracy of the Mars gravity potential model used to determine the spacecraft's orbit.

Mariner 9 approached the surface of Mars closely enough to be sensitive to the higher-degree terms in the spherical-harmonic expansion of Mars' gravitational potential. Experiences with artificial satellites of the earth and with lunar orbiters have demonstrated the difficulties inherent in the determination of reliable coefficients in this expansion from the analysis of radio-tracking data from numerous spacecraft in diverse orbits and a fortiori from one spacecraft with a fixed periapse latitude.

Nevertheless, the development by one of us (RDR) of a limited-memory filter, feasible economically for use in the analysis of the Mariner-9 data, has allowed us to obtain a reliable, complete, sixth-degree model of this expansion of Mars' gravitational potential. The heights of the corresponding equipotential near the surface of Mars are estimated, as described below, to be uncertain by no more than about 100 m for the region below 60° North Latitude. For higher latitudes the uncertainties increase to about 300m.

This model represents a significant improvement over those discussed previously (Lorell et al., 1973). These earlier models exhibited unrealistically large undulations in the northern hemisphere, in part because the periapse of Mariner 9 was located at about 23° South Latitude. These artifacts were also due partly to the use of data sets with uneven longitude coverage and to the use of a less effective filter. They persisted even when fairly strong a priori constraints were placed on the coefficients in the harmonic expansion.

Our approach, which utilizes more uniform longitude coverage, takes advantage of both the short-period effects of the gravity field, manifested primarily through the tracking data obtained near periapse passages, and the long-period and secular effects which accumulate over many satellite orbital revolutions. Other approaches that have been used recently concentrated exclusively either on the data obtained near periapse (Sjogren et al., 1975) or on the long-term and secular effects (Born, 1974).

Method of Analysis

The data utilized in our analysis comprised six disjoint 19-day spans, covering the periods from 16 Nov 71 to 23 Dec 71, and from 6 Jan 72 to 22 Mar 72. These data were the best available from the points of view of continuity of tracking and, to a lesser extent, of signal-to-noise ratio. Each of these 19-day spans corresponded to a "resonance period" in which the sub-periapse point of Mariner 9 completes a cycle in longitude.

Because of the presence of important random, or quasi-random, accelerations of the spacecraft, due, for example, to imbalances in the gas jets used to control the orientation of the spacecraft (see Figure 1 in Lorell et al., 1973), it is not fruitful to process the data in the usual "batch" mode least-squares analysis. Approximations to the Kalman-Bucy filter (Jazwinski, 1970) were therefore used.

The six resonance spans were divided

into three sets of two spans each, the first two sets being composed of alternate members of the first four spans. Each set was analyzed separately and with two different filters. The first, a dual-span filter (DSF), consisted of the estimation, by weighted least squares, of the appropriate set of coefficients of the spherical-harmonic expansion (Appendix A), and of two spacecraft state vectors, one for each data span. The second, a limited-memory filter (LMF), involved the estimation of the same set of coefficients but twice the number of spacecraft state vectors, one for each 9.5 days of data. In all cases, parameters describing such quantities as the mass of Mars, the direction of its rotation axis, the location on the earth of the tracking stations, and the radiation pressure exerted on the spacecraft, were fixed in accord with prior determinations. All solutions were of full rank and complete in the harmonic expansion to the particular degree chosen, except that the coefficients C_{21} and S_{21} were held at zero. No a priori constraint was used, either for the other coefficients or for the spacecraft state.

The three models produced with a given filter for a given degree were intercompared through contour maps. For each model, a map (DMEPS) was formed by taking the difference of the heights of the equipotential surface (EPS) for that model and the mean of the corresponding heights for all three models. The contours, which had a separation of 25 m, were examined in each of two latitude regions: 70°S to 30°N and 70°S to 65°N. A study in these overlapping zones was chosen in lieu of a more formal analysis because the EPS height errors do not have well understood statistics. The "greatest deviation" and the "typical deviation" were recorded for each region of each DMEPS plot. These numbers showed that the LMF yielded significantly more consistent models, especially for those of higher degree.

Intercomparisons of the LMF solutions for the spherical harmonic models of 6th, 7th, and 8th degree led to the conclusion that the highest resolution model that our analysis can support is of sixth degree. This model was found to be similar to, and apparently slightly more reliable than, the 7th-degree model. The two triads of 8th-degree models proved highly disparate.

The post-fit rms residuals for the 6th-degree LMF models were under 0.25 Hz. This was, of course, lower than the corresponding DSF number because of the larger number of parameters adjusted in the LMF. By dividing the data into sufficiently short arcs it should be possible to bring the residuals quite close to the nominal noise level of under 0.01 Hz. However, we do not expect that this procedure would produce a substantially better estimate of the gravity field.

To obtain our final model of the gravity field we used the simple and adequate procedure of averaging arithmetically the means of the coefficients of the 6th-degree models obtained with the LMF. These means are shown in Table 1. Figure 1 shows the equipotential surface corresponding to this mean model with J_2 set to zero. The DMEPS plots corresponding to this 6th-degree model were examined in greater detail in order to estimate the uncertainty in the EPS heights. The local extrema below 60°N, obtained from contours with 25 m separation, have 1) a mean absolute value of 95 m; 2) a mode and median absolute value of 75 m; and 3) an rms of 110 m. From these statistics we estimate that the EPS shown in Figure 1 is reliable to about 100 m below

Table 1. Coefficients for Spherical-Harmonic Expansion of the Gravitational Potential of Mars*

C_{21}	≡ 0.0	S_{53}	= -0.029
S_{21}	≡ 0.0	C_{54}	= -0.132
C_{22}	= -0.841	S_{54}	= -0.032
S_{22}	= 0.494	C_{55}	= -0.051
C_{31}	= 0.047	S_{55}	= 0.036
S_{31}	= 0.261	C_{61}	= 0.027
C_{32}	= -0.163	S_{61}	= -0.015
S_{32}	= 0.079	C_{62}	= 0.058
C_{33}	= 0.358	S_{62}	= 0.012
S_{33}	= 0.249	C_{63}	= 0.018
C_{41}	= 0.052	S_{63}	= -0.019
S_{41}	= 0.037	C_{64}	= -0.026
C_{42}	= -0.003	S_{64}	= 0.081
S_{42}	= -0.116	C_{65}	= 0.006
C_{43}	= 0.064	S_{65}	= 0.020
S_{43}	= -0.021	C_{66}	= 0.023
C_{44}	= -0.005	S_{66}	= 0.016
S_{44}	= -0.168	J_2	= 19.550
C_{51}	= 0.013	J_3	= 0.113
S_{51}	= 0.032	J_4	= -0.573
C_{52}	= -0.015	J_5	= -0.452
S_{52}	= -0.012	J_6	= -0.665
C_{53}	= 0.027		

* Each coefficient has been multiplied by 10^4 ; see Appendix for relevant definitions. We note that for the model given by Lorell et al. (1973), the second degree terms, normalized as above, are $J_2 = 19.6$, $C_{22} = -0.79$, and $S_{22} = 0.53$.

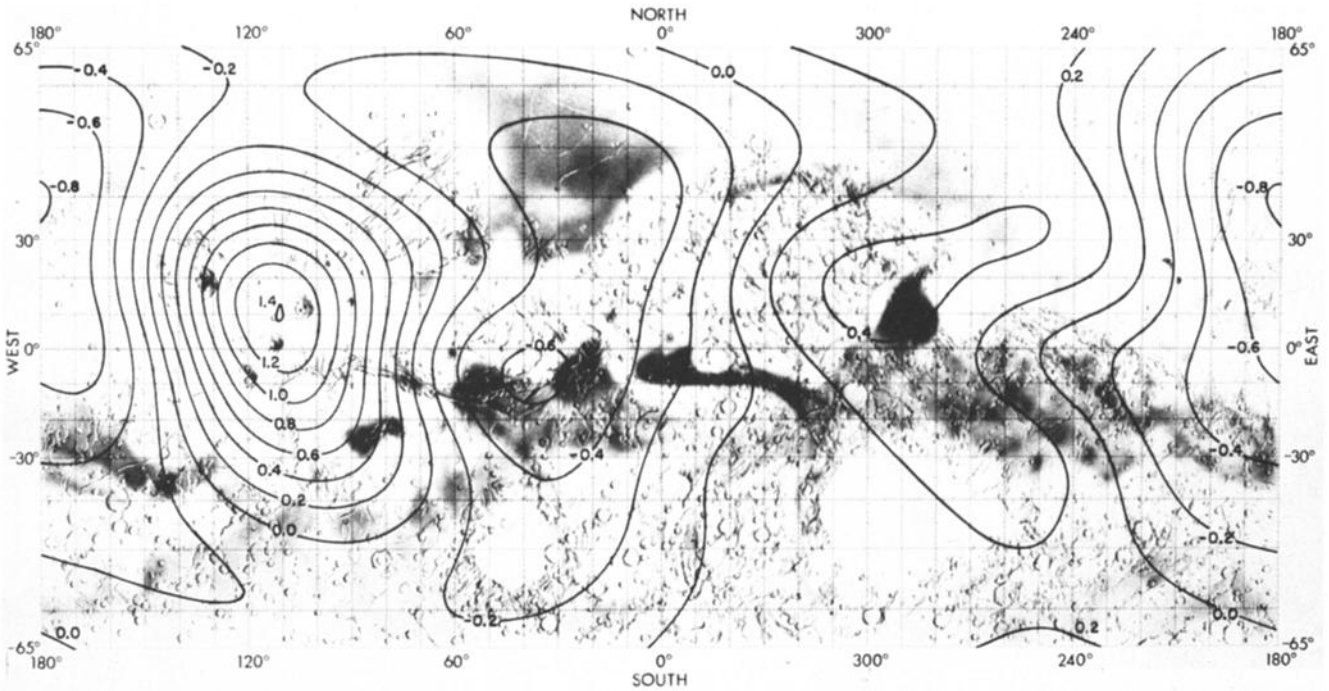

Figure 1. Contour map for an equipotential surface of Mars' gravity field superposed on a montage of photographs of the surface, provided by H. Masursky, courtesy of the United States Geological Survey. The contours omit the effects of J_2 and are referred to a radius of 3394 km. Contours are shown at 0.2 km intervals. A Mercator projection is shown.

60°N. Of course, the rms of the extrema should be substantially larger than the rms errors of the contour in Figure 1; in addition, some advantage is presumably gained by averaging the three separate sets of coefficients. However, the possibility of systematic effects, common to all three LMF solutions, despite each being dependent on a totally different data set, requires that we not make a smaller estimate of the uncertainty. By a similar method we assign uncertainties of up to 300 m for the EPS heights above 60°N.

Sjogren et al.(1975) have recently developed a Mars gravity model with EPS height uncertainties "ranging from 60 m near the equator to 500 m at the poles." We have compared this model to ours by plotting contours of the difference EPS with 25 m separation. An examination of the extrema of these contours below 60°N yields: 1) a mean absolute of 120 m; 2) mode and median absolutes of 100 m; and 3) an rms of 135 m. For the region below 30°N the rms drops to 100 m. Above 60°N the difference contours are dominated by a single feature that reaches 450 m at the pole. We find this agreement highly satisfactory considering that the models were generated by different analysis methods and disjoint sets of data.

Discussion

The equipotential surface of Mars (Figure 1) is clearly dominated by the rise in the region of Tharsis, 105° West Longitude. The other major elevated region of the equipotential surface, near 285° West Longitude, and the depressed areas in between all seem to be manifestations of the Tharsis construct. The indentations of the contour lines that appear on the East side of Tharsis are probably associated with the Valles Marineris (Sjogren et al., 1975).

Shallow structures in the EPS tend to be obscured by the Tharsis-related undulations. By offsetting the center of the spheroid used as reference for the EPS, this obscuring effect can be reduced. (A possible geophysical basis for this approach will be discussed in a separate publication.) In such an "offset-contour" plot, the Hellas depression, as well as the Valles Marineris, appear as gravitational "lows". There seems to be a pattern of undercompensation for major surface features (Christensen, 1975). Such undercompensation is consistent with the assertion that the Martian lithosphere must be thick (approximately 200 km) and rigid (Carr, 1974), and thus able to support a substantial disequilibrium.

Appendix

The spherical-harmonic expansion of the gravitational potential of Mars is written as

$$U = -\frac{GM_\sigma}{r}\left\{1 - \sum_{n=2}^{\infty} J_n \left(\frac{a}{r}\right)^n P_n(\sin\theta) +\right.$$

$$\sum_{n=2}^{\infty} \sum_{m=1}^{n} \left(\frac{a}{r}\right)^n P_{nm}(\sin\theta) \cdot$$

$$[C_{nm}\cos m\lambda + S_{nm}\sin m\lambda]\}; \quad r > a,$$

where P_n and P_{nm} are, respectively, the Legendre and associated Legendre polynomials; a = 3394 km is the value assumed for the equatorial radius of Mars; $M_\sigma = (3098700)^{-1} M_\odot$ is the mass of Mars with $M_\odot$ the mass of the sun; G is the universal constant of gravitation; r, θ, and λ are the usual Mars-centered coordinates: radius, latitude, and longitude, referred to a pole of rotation defined by right ascension 317°.28 and declination 52°.77 (1950.0); and the J_n, C_{nm}, and S_{nm} are the coefficients to be estimated with the normalization defined by

$$\int_{-1}^{1} P_n^2(x)dx = 2(2n+1)^{-1}; \quad \int_{-1}^{1} P_{nm}^2(x)dx = 4.$$

Acknowledgements. We thank M. E. Ash and G. L. Slater for their important contributions to the early phases of our research, J. Lorell, J. F. Jordan, and other members of the staff of the Jet Propulsion Laboratory for their indispensable cooperation, and the computation group at the Charles Stark Draper Laboratory, Inc., for their cooperation in the processing of the data. This research was supported by a grant from the National Aeronautics and Space Administration, NGR 22-009-804.

References

Born, G. H., Mars Physical Parameters as Determined from Mariner 9 Observations of the Natural Satellites and Doppler Tracking, J. Geophys. Res. 78, 4837-4844, 1974.

Carr, M. H., Tectonism and Volcanism of the Tharsis Region of Mars, J. Geophys. Res. 79, 3943-3949, 1974.

Christensen, E. J., Martian Topography Derived from Occultation, Radar, Spectral and Optical Measurements, submitted to J. Geophys. Res., 1975.

Jazwinski, A. H., Stochastic Processes and Filtering Theory, pp. 189-193, Academic Press, New York, 1970.

Johnston, D. H., McGetchin, T. R. and Toksoz, M. N., The Thermal State and Internal Structure of Mars, J. Geophys. Res. 79, 3959-3971, 1974.

Lorell, J., Born, G. H., Christensen, E. J., Esposito, P. B., Jordan, J. F., Laing, P. A., Sjogren, W. L., Wong, S. K., Reasenberg, R. D., Shapiro, I. I. and Slater, G. L., Gravity Field of Mars from Mariner 9 Tracking Data, Icarus 18, 304-316, 1973.

Sjogren, W. L., Lorell, J., Wong, L. and Downs, W., Mars Gravity Field Based on a Short-Arc Technique, J. Geophys. Res., 1975.

(Received January 17, 1975;
accepted February 6, 1975.)